31st Annual International Conference of the IEEE EMBS
Minneapolis, Minnesota, USA, September 2-6, 2009

Pulse Pressure Variation Estimation Using a Sequential Monte Carlo Method

Sunghan Kim[1], Mateo Aboy[2], and James McNames[1]

***Abstract*— We describe a novel automatic algorithm to continuously estimate the pulse pressure variation (PPV) index from arterial blood pressure (ABP) signals. The algorithm utilizes our recently developed sequential Monte Carlo method (SMCM) based on a maximum *A-Posterior* adaptive marginalized particle filter (MAM-PF). The PPV index is one of most specific and sensitive dynamic indicators of fluid responsiveness in mechanically ventilated patients. We report the assessment results of the proposed algorithm on real ABP signals.**

***Index Terms*— Amplitude modulation, amplitude modulation index, pulse pressure variation, sequential Monte Carlo method, state-space model.**

I. Introduction

In many critical care settings clinicians must decide whether patients should be given intravenous fluid boluses and other therapies to improve perfusion. This is a critical tradeoff because excessive fluid can impair lung function thereby decreasing oxygen delivery to tissues and ultimately contributing to organ failure. However, low perfusion caused by insufficient fluid can also lead to tissue damage. Determining the best course of fluid therapy for a patient is difficult and clinicians have few clinical signs to guide them.

The pulse pressure variation (PPV) index is a measure of the respiratory effect on the variation of systemic arterial blood pressure in patients receiving full mechanical ventilation [1]–[5]. It is a promising predictor of who will have a significant increase in cardiac output due to an infusion of fluid. We describe a novel automatic algorithm that can be used to obtain the pulse pressure variation (PPV) index from arterial blood pressure (ABP) signals. The proposed algorithm is based on sequential Monte Carlo estimation methods.

The standard method for calculating PPV often requires simultaneous recording of arterial and airway pressure. Pulse pressure (PP) is manually calculated on a beat-to-beat basis as the difference between systolic and diastolic arterial pressure. Maximal PP ($\mathrm{PP}_{\max}$) and minimal PP ($\mathrm{PP}_{\min}$) are calculated over a single respiratory cycle, which is determined from the airway pressure signal. Pulse pressure variation, ΔPP, is then calculated as the percentage

$$\Delta\mathrm{PP}(\%) = 100 \times \frac{\mathrm{PP}_{\max} - \mathrm{PP}_{\min}}{(\mathrm{PP}_{\max} + \mathrm{PP}_{\min})/2} \tag{1}$$

This work was supported in part by the Thrasher Research Fund.
[1]Sunghan Kim (corresponding author, sunghan@pdx.edu) and James McNames (director, mcnames@pdx.edu) are with Biomedical Signal Processing Laboratory at Portland State University
[2]Mateo Aboy (mateoaboy@ieee.org) is with Electrical Engineering Department at Oregon Institute of Technology

There are few publicly available algorithms to automatically estimate PPV accurately and reliably. We have previously described a beat detection-based PPV algorithm [6]. This previous algorithm was made publicly available by the authors and it has been adopted by Philips Medical Systems. Currently, our previously published PPV index is displayed in real-time on the Philips Intellivue MP70 monitors (Intellivue MP70, Philips Medical Systems). Its ability to monitor fluid responsiveness in the operating room and its accuracy against the gold standard obtained by manual annotations were assessed by Cannesson [7].

A limitation of our previously described [6] algorithm adopted by Philips in their Intellivue MP70 monitors is that it may not work adequately in regions of abrupt hemodynamic changes. In this paper, we describe an improved algorithm capable of continuously estimating PPV based on a maximum *A-Posterior* adaptive marginalized particle filter (MAM-PF).

II. Algorithm Description

The proposed PPV index tracker utilizes our recently developed MAM-PF which is based on the state-space model approach. The state-space method is a tool to describe the evolution of an unobservable state $\boldsymbol{x}_n$ and its relation to measurement $\boldsymbol{y}_n$ so that one can estimate $\boldsymbol{x}_n$ as a function of $\boldsymbol{y}_n$. The typical state-space model can be expressed as,

$$\boldsymbol{x}_{n+1} = f(\boldsymbol{x}_n) + \boldsymbol{u}_n \tag{2}$$
$$\boldsymbol{y}_n = h(\boldsymbol{x}_n) + \boldsymbol{v}_n \tag{3}$$

where (2) is a process model, (3) a measurement model, $f(\cdot)$ and $h(\cdot)$ nonlinear functions of the ℓ dimensional state $\boldsymbol{x}_n$, and $\boldsymbol{u}_n$ and $\boldsymbol{v}_n$ uncorrelated white noise with variances q and r, respectively. $\hat{\boldsymbol{x}}_{n|0:n}$ denotes a causal estimate of $\boldsymbol{x}_n$ given all previous measurements $\boldsymbol{y}_{0:n} = \{\boldsymbol{y}_0, \ldots, \boldsymbol{y}_n\}$. The proposed PPV index tracker produces a causal estimate $\hat{\boldsymbol{x}}_{n|0:n}$, so that it can be implemented as a real-time application. However, the tracker is easily generalized to produce non-causal estimates for offline analysis in which the entire recording is available.

A. Notation

We have adopted the notation used in [8] with minor modification. We used boldface to denote random processes, normal face for deterministic parameters and functions, upper case letters for matrices, lower case letters for vectors and scalars, and subscripts for time indices.

B. Measurement Model

McNames *et al.* proposed a general measurement model of the cardiovascular signal [9]. However, their model is not appropriate to estimate the PPV index. We propose a novel measurement model of the ABP signal, from which one can obtain the PPV index directly with minimal computation. The measurement model is shown in (4)–(8),

$$\boldsymbol{y}_n = \boldsymbol{s}_n + \boldsymbol{v}_n \tag{4}$$

$$\boldsymbol{s}_n = \boldsymbol{r}_n + (1 + \boldsymbol{m}_n)\, \boldsymbol{c}_n + \boldsymbol{t}_n \tag{5}$$

$$\boldsymbol{r}_n = \sum_{k=1}^{N_{\mathrm{h}}^{\mathrm{r}}} \boldsymbol{c}_{1,k,n} \cos\left(k\boldsymbol{\theta}_n^{\mathrm{r}}\right) + \boldsymbol{c}_{2,k,n} \sin\left(k\boldsymbol{\theta}_n^{\mathrm{r}}\right) \tag{6}$$

$$\boldsymbol{m}_n = \sum_{k=1}^{N_{\mathrm{h}}^{\mathrm{r}}} \boldsymbol{c}_{3,k,n} \cos\left(k\boldsymbol{\theta}_n^{\mathrm{r}}\right) + \boldsymbol{c}_{4,k,n} \sin\left(k\boldsymbol{\theta}_n^{\mathrm{r}}\right) \tag{7}$$

$$\boldsymbol{c}_n = \sum_{k=1}^{N_{\mathrm{h}}^{\mathrm{c}}} \boldsymbol{c}_{5,k,n} \cos\left(k\boldsymbol{\theta}_n^{\mathrm{c}}\right) + \boldsymbol{c}_{6,k,n} \sin\left(k\boldsymbol{\theta}_n^{\mathrm{c}}\right) \tag{8}$$

where $\boldsymbol{r}_n$ is a respiratory signal, $\boldsymbol{m}_n$ a modulation factor, $\boldsymbol{c}_n$ a cardiac signal, $\boldsymbol{t}_n$ a slow signal trend, $\boldsymbol{\theta}_n^{\mathrm{r}}$ a respiratory instantaneous angle, $\boldsymbol{\theta}_n^{\mathrm{c}}$ a cardiac instantaneous angle, $N_{\mathrm{h}}^{\mathrm{r}}$ the number of respiratory harmonic components, $N_{\mathrm{h}}^{\mathrm{c}}$ the number of cardiac harmonic components, and $\boldsymbol{v}_n$ a white Gaussian observation noise with variance r. The amplitude of the modulation factor $\boldsymbol{m}_n$ represents the degree of the amplitude modulation (AM) of the cardiac signal $\boldsymbol{c}_n$ due to the respiratory signal $\boldsymbol{r}_n$. In the proposed model $\boldsymbol{m}_n$ is modeled as a separate component from $\boldsymbol{r}_m$ although both reflect the respiratory activity. However, in the general cardiovascular model proposed by McNames *et al.*, $\boldsymbol{m}_n$ is modeled as a filtered quantity of $\boldsymbol{r}_n$, which makes it hard to compute PPV directly from the model. Given the measurement model shown in (4)–(8) the total number of parameters to estimate is $4N_{\mathrm{h}}^{\mathrm{r}} + 2N_{\mathrm{h}}^{\mathrm{c}} + 2$.

C. Process Model

In many applications the range of the possible mean frequencies is known from domain knowledge. For example, in an application to track the heart rate of an adult, the range of typical adult heart rates is known. We model this by designing the process model such that $\bar{\boldsymbol{f}}_n$ has a uniform distribution $\bar{f} \sim \mathcal{U}(f_{\min}, f_{\max})$. The process model can be written as,

$$\bar{\boldsymbol{f}}_{n+1}^{\mathrm{c}} = g\left[\bar{\boldsymbol{f}}_n^{\mathrm{c}} + \boldsymbol{u}_{\bar{\boldsymbol{f}}^{\mathrm{c}},n}\right] \tag{9}$$

$$\boldsymbol{f}_{n+1}^{\mathrm{c}} = \bar{\boldsymbol{f}}_n^{\mathrm{c}} + \alpha\left(\boldsymbol{f}_n^{\mathrm{c}} - \bar{\boldsymbol{f}}_n^{\mathrm{c}}\right) + \boldsymbol{u}_{\boldsymbol{f},n} \tag{10}$$

$$\boldsymbol{\theta}_{n+1}^{\mathrm{c}} = \boldsymbol{\theta}_n^{\mathrm{c}} + 2\pi T_{\mathrm{s}} \boldsymbol{f}_n^{\mathrm{c}} \tag{11}$$

where $g\left[\cdot\right]$ is a nonlinear reflecting function,

$$g[f] = \begin{cases} f_{\max} - (f - f_{\max}) & f_{\max} < f \\ f & f_{\min} < f \leq f_{\max} \\ f_{\min} + (f_{\min} - f) & f \leq f_{\min} \end{cases} \tag{12}$$

This essentially causes the mean frequency $\bar{\boldsymbol{f}}_n^{\mathrm{c}}$ to bounce elastically from the boundaries at $f_{\max}$ and $f_{\min}$, which in turn ensures that at any given time n the mean frequency $\bar{\boldsymbol{f}}^{\mathrm{c}}$ is uniformly distributed within this range. The respiratory rate $\boldsymbol{f}_n^{\mathrm{r}}$ is a known constant value $\boldsymbol{f}^{\mathrm{r}}$ since the ABP signal is from mechanically ventilated subjects in which the clinician specifies the respiratory rate. The respiratory instantaneous angle $\boldsymbol{\theta}_{n+1}^{\mathrm{r}}$ can be expressed as a cumulative sum of $\boldsymbol{f}^{\mathrm{r}}$, which can be written as,

$$\boldsymbol{\theta}_{n+1}^{\mathrm{r}} = 2\pi(n+1)T_{\mathrm{s}}\boldsymbol{f}^{\mathrm{r}}. \tag{13}$$

The sinusoidal coefficients $\{\boldsymbol{c}_{1,k,n}, \ldots, \boldsymbol{c}_{6,k,n}\}$ and the slow signal trend $\boldsymbol{t}_n$ are modeled as random walk processes,

$$\boldsymbol{c}_{\cdot,k,n+1} = \boldsymbol{c}_{\cdot,k,n} + \boldsymbol{u}_{\boldsymbol{c},n} \tag{14}$$

$$\boldsymbol{t}_{k,n+1} = \boldsymbol{t}_n + \boldsymbol{u}_{\boldsymbol{t},n} \tag{15}$$

where $\boldsymbol{u}_{\boldsymbol{c}_{\cdot},n}$ and $\boldsymbol{u}_{\boldsymbol{t},n}$ are white Gaussian process noises with variances $q_{\boldsymbol{c}_{\cdot}}$ and q_t, respectively.

TABLE I

SUMMARY OF USER-SPECIFIED DESIGN PARAMETERS FOR THE PPV INDEX TRACKER

Name	Symbol	Value
No. particles	N^{p}	250
No. cardiac harmonic components	$N_{\mathrm{h}}^{\mathrm{c}}$	6
No. respiratory harmonic components	$N_{\mathrm{h}}^{\mathrm{r}}$	3
Minimum heart rate	$f_{\min}^{\mathrm{c}}$	60/60 Hz
Maximum heart rate	$f_{\max}^{\mathrm{c}}$	140/60 Hz
Measurement noise variance	r	σ_y/1000
Cardiac mean frequency variance	$q_{\bar{f}^{\mathrm{c}}}$	7e-6 T_{s}
Cardiac frequency variance	$q_{f^{\mathrm{c}}}$	7e-4 T_{s}
Respiratory signal coefficient variance	q_{c_1}&q_{c_2}	1e-5 T_{s}
Modulation factor coefficient variance	q_{c_3}&q_{c_4}	1e-9 T_{s}
Cardiac signal coefficient variance	q_{c_5}&q_{c_6}	1e-6 T_{s}

D. ABP Signal Tracking

We proposed a multiharmonic tracking method based on the conventional sequential Monte Carlo method (SMCM) [10]. Recently we have developed a novel SMCM that can overcome some of the limitations of conventional SMCM algorithms such as sample degeneracy, sample impoverishment, and multi-modal posterior distributions [11]. We applied the new SMCM, called the maximum *a posteriori* adaptive marginalized particle filter (MAM-PF), to the state-space model of the ABP signal. The MAM-PF is able to track the heart rate $\boldsymbol{f}_n^{\mathrm{c}}$ along with other sinusoidal coefficients $\{\boldsymbol{c}_{1,k,n}, \ldots, \boldsymbol{c}_{6,k,n}\}$ and the slow signal trend $\boldsymbol{t}_n$.

Table I lists the MAM-PF ABP signal tracker's user-specified parameters such as the number of particles, the number of harmonic components, process and measurement noise variances, and initial values.

E. PPV Tracking

The PPV index (ΔPP) is the peak-to-peak value of the modulation factor $\boldsymbol{m}_n$ as shown in Fig. 1. It is also $2\times$ the AM modulation index of the amplitude-modulated cardiac signal, $(1 + \boldsymbol{m}_n)\, \boldsymbol{c}_n$. Given the estimated sinusoidal

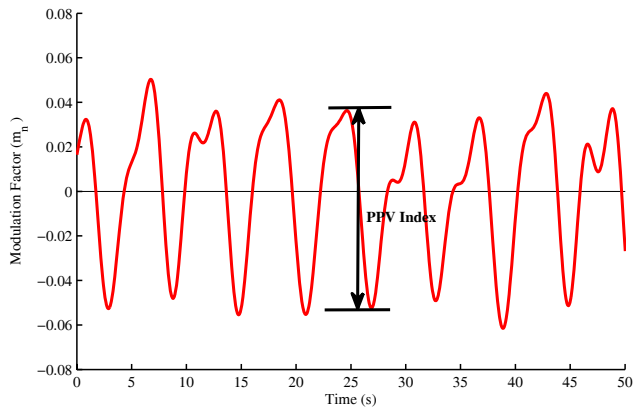

Fig. 1. Modulation factor $\boldsymbol{m}_n$ and PPV index ΔPP

coefficients $\{\boldsymbol{c}_{3,k,n}, \boldsymbol{c}_{4,k,n}\}$, the modulation factor's peak-to-peak value $\Delta\boldsymbol{m}_n$ can be easily estimated as follows,

$$\begin{aligned}
\boldsymbol{\theta}_{\max} &= \arg\max_{\theta} \sum_{k=1}^{N_{\mathrm{h}}^{\mathrm{r}}} \boldsymbol{c}_{3,k,n}\cos(k\theta) + \boldsymbol{c}_{4,k,n}\sin(k\theta) \\
\boldsymbol{\theta}_{\min} &= \arg\min_{\theta} \sum_{k=1}^{N_{\mathrm{h}}^{\mathrm{r}}} \boldsymbol{c}_{3,k,n}\cos(k\theta) + \boldsymbol{c}_{4,k,n}\sin(k\theta) \\
\boldsymbol{m}_{n,\max} &= \sum_{k=1}^{N_{\mathrm{h}}^{\mathrm{r}}} \boldsymbol{c}_{3,k,n}\cos(k\boldsymbol{\theta}_{\max}) + \boldsymbol{c}_{4,k,n}\sin(k\boldsymbol{\theta}_{\max}) \\
\boldsymbol{m}_{n,\min} &= \sum_{k=1}^{N_{\mathrm{h}}^{\mathrm{r}}} \boldsymbol{c}_{3,k,n}\cos(k\boldsymbol{\theta}_{\min}) + \boldsymbol{c}_{4,k,n}\sin(k\boldsymbol{\theta}_{\min}) \\
\Delta\boldsymbol{m}_n &= \boldsymbol{m}_{n,\max} - \boldsymbol{m}_{n,\min}
\end{aligned} \tag{16}$$

where $100 \times \Delta\boldsymbol{m}_n$ is equal to ΔPP(%). Aboy *et al.* proposed an algorithm to estimate the PPV index based on bandpass-filtering, beat detection, and interpolation [6]. Our PPV index estimation method does not involve any filtering process or beat detection algorithm which is prone to noise.

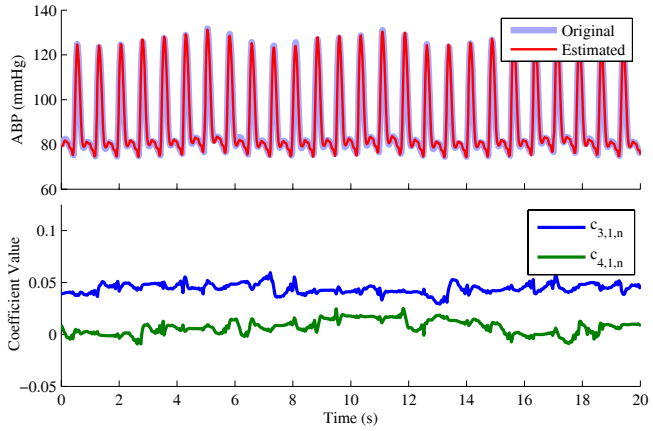

Fig. 2. Original and estimate ABP signals (top) and sinusoidal coefficients $\{\boldsymbol{c}_{3,1,n}, \boldsymbol{c}_{4,1,n}\}$ of the modulation factor $\boldsymbol{m}_n$ (bottom)

III. Assessment

A. Data Collection

The Massachusetts General Hospital (MGH) Waveform Database on PhysioNet is a comprehensive collection of electronic recordings of hemodynamic and electrocardiographic waveforms patients in critical care units [12], [13]. The database includes ABP signals in addition to seven other types of waveforms. By visual inspection of the spectrogram of ABP signals we identified two patients whose ABP signals were clean and respiratory rate remained constant at least for 10 consecutive minutes. We used the constant respiratory rate shown in spectrogram as an indicator of full respiratory support.

Since the respiratory rate $\boldsymbol{f}^{\mathrm{r}}$ was not annotated or recorded as part of this data set, we estimated it from the ABP signal in three steps. First, the ABP signal was lowpass-filtered with a cutoff frequency of 1 Hz to remove all cardiac components. Second, multiple synthetic cosine signals $\cos(2\pi n T_{\mathrm{s}} f)$ were generated by sweeping the frequency f from 0.01 to 1. Finally, we calculated cross-correlation between the lowpass-filtered ABP signal and synthetic cosine signals and chose the frequency that maximized the correlation as our estimated respiratory rate $\boldsymbol{f}^{\mathrm{r}}$.

B. Gold Standard

We manually detected the peaks and troughs of the ABP signals and calculated the PPV indices, which is the best current practice. They are referred to as manual PPV indices. A Bland-Altman plot is a visualization method that is often used in PPV index estimation to determine the agreement between two different estimates. We used it to compare the best current practice using manual annotations with our new automatic tracking algorithm.

IV. Results and Discussion

Fig. 2 shows an example of the original and estimated ABP signals (top) and sinusoidal coefficients $\{\boldsymbol{c}_{3,1,n}, \boldsymbol{c}_{4,1,n}\}$ of the fundamental component of the modulation factor $\boldsymbol{m}_n$ (bottom). Given the sinusoidal coefficients $\{\boldsymbol{c}_{3,k,n}, \boldsymbol{c}_{4,k,n}\}$, the PPV index ΔPP can be obtained as explained in (16).

Figs. 3 and 4 illustrate the time series of manual and automatic PPV indices (top) and Bland-Altman plot (bottom) of each of two patients. The PPV indices of the first patient were relatively smaller (under 30%) than those (over 30%) of the second patient. The variation of the first patient's PPV indices was also smaller than that of the second patient's. In both cases, the proposed method was able to estimate the PPV index accurately over a wide range of the manual PPV index. Table II lists the percentage of the automatic PPV indices within a certain estimation error range.

There is a slight delay in the automatic PPV index estimates as compared to the manual estimates because the automatic algorithm is causal and only uses past and present observations of the ABP signal to estimate the PPV index. The manual estimates are based on non-causal estimates of the systolic and diastolic peaks and therefore lacks the slight delay observed with the automatic algorithm. For offline

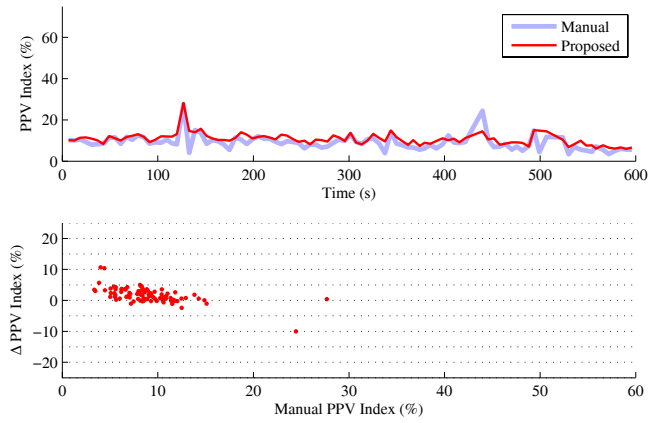

Fig. 3. Time series of manual and automatic PPV indices (top) and Bland-Altman plot (bottom) of Patient 1

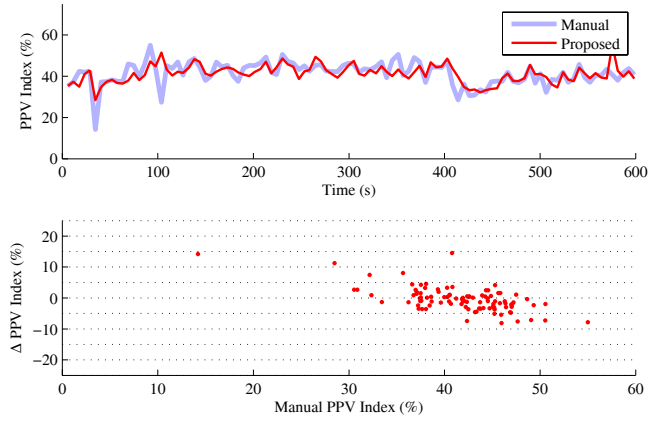

Fig. 4. Time series of manual and automatic PPV indices (top) and Bland-Altman plot (bottom) of Patient 2

signal analysis, the proposed tracking algorithm could easily be modified to produce non-causal estimates with improved accuracy and no delay.

V. Summary

We proposed a novel state-space model of the ABP signal from which one can obtain the PPV index directly and continuously. We adopted our recently developed multiharmonic tracking method to estimate the parameters of this state-space model. Using the estimated parameters we devised a novel way to estimate the PPV index without involving any filtering or beat detection.

Commercial devices for PPV monitoring are still under development and the estimates provided by the current generation of devices are not always accurate. The automatic algorithm described in this paper uses a new approach with greater accuracy that may ultimately improve the outcome of people with critical injuries and illness by helping clinicians more accurately predict the response to fluid therapy.

VI. Acknowledgement

This work was made possible through funding from Thrasher Research Fund and the Medical Research Fund of Oregon. We are grateful for their financial support.

TABLE II

Summary of performance measure of the PPV index tracker

Δ PPV Index (%)	Patient1 (%)	Patient2 (%)
± 5	94	91
± 10	97	96
± 15	100	100

References

[1] F. Michard, S. Boussat, D. Chemla, N. Anguel, A. Mercat, Y. Lecarpentier, C. Richard, M. R. Pinsky, and J. L. Teboul, "Relation between respiratory changes in arterial pulse pressure and fluid responsiveness in septic patients with acute circulatory failure.," American Journal of Respiratory and Critical Care Medicine, vol. 162, no. 1, pp. 134–8, Jul 2000.

[2] F. Michard, L. Ruscio, and J. L. Teboul, "Clinical prediction of fluid responsiveness in acute circulatory failure related to sepsis.," Intensive Care Medicine, vol. 27, no. 7, pp. 1238, Jul 2001.

[3] Frdric Michard and Jean-Louis Teboul, "Predicting fluid responsiveness in ICU patients: a critical analysis of the evidence.," Chest, vol. 121, no. 6, pp. 2000–8, Jun 2002.

[4] Andreas Kramer, David Zygun, Harvey Hawes, Paul Easton, and Andre Ferland, "Pulse pressure variation predicts fluid responsiveness following coronary artery bypass surgery.," Chest, vol. 126, no. 5, pp. 1563–8, Nov 2004.

[5] C. K. Hofer, L. Furrer, S. Matter-Ensner, M. Maloigne, R. Klaghofer, M. Genoni, and A. Zollinger, "Volumetric preload measurement by thermodilution: a comparison with transoesophageal echocardiography.," Br J Anaesth, vol. 94, no. 6, pp. 748–55, Jun 2005.

[6] M. Aboy, J. McNames, T. Thong, C.R. Phillips, M.S. Ellenby, and B. Goldstein, "A novel algorithm to estimate the pulse pressure variation index," IEEE Transactions on Biomedical Engineering, vol. 51, pp. 2198–2203, 2004.

[7] Maxime Cannesson, Juliette Slieker, Olivier Desebbe, Christian Bauer, Pascal Chiari, Roland Hnaine, and Jean-Jacques Lehot, "The ability of a novel algorithm for automatic estimation of the respiratory variations in arterial pulse pressure to monitor fluid responsiveness in the operating room.," Anesth Analg, vol. 106, no. 4, pp. 1195–200, table of contents, Apr 2008.

[8] Olivier Cappé, Simon Godsill, and Eric Moulines, "An overview of existing methods and recent advances in sequential Monte Carlo," in Proceedings of the IEEE. May 2007, vol. 95, pp. 899–924, IEEE-INST ELECTRICAL ELECTRONICS ENGINEERS INC.

[9] J. McNames and M. Aboy, "Statistical modeling of cardiovascular signals and parameter estimation based on the extended kalman filter," IEEE Transactions on Biomedical Engineering, vol. 55, no. 1, pp. 119–129, Jan. 2008.

[10] Sunghan Kim, Lars Holmstrom, and James McNames, "Multiharmonic Tracking Using Marginalized Particle Filters," in 30th Annual International Conference of the IEEE Engineering in Medicine and Biology Society - Proceedings, Aug. 2008, pp. 29–33.

[11] S. Kim, L. Holmstrom, and J. McNames, "The maximum a posteriori adaptive marginalized particle filter," Submitted to Transactions on Signal Processing.

[12] A. L. Goldberger, L. A. N. Amaral, L. Glass, J. M. Hausdorff, P. Ch. Ivanov, R. G. Mark, J. E. Mietus, G. B. Moody, C.-K. Peng, and H. E. Stanley, "PhysioBank, PhysioToolkit, and PhysioNet: Components of a new research resource for complex physiologic signals," Circulation, vol. 101, no. 23, pp. e215–e220, Jun. 2000, Circulation Electronic Pages: http://circ.ahajournals.org/cgi/content/full/101/23/e215.

[13] G. B. Moody and R. G. Mark, "A database to support development and evaluation of intelligent intensive care monitoring," Computers in Cardiology, vol. 23, pp. 657–660, 1996.